NASA/TM—2008-215492

The Effect of Simulated Lunar Dust on the Absorptivity, Emissivity, and Operating Temperature on AZ–93 and Ag/FEP Thermal Control Surfaces

James R. Gaier and John Siamidis
Glenn Research Center, Cleveland, Ohio

Scott R. Panko
Arctic Slope Research Corporation, Cleveland, Ohio

Kerry J. Rogers
Manchester College, North Manchester, Indiana

Elizabeth M.G. Larkin
Case Western Reserve University, Cleveland, Ohio

December 2008

NASA STI Program . . . in Profile

Since its founding, NASA has been dedicated to the advancement of aeronautics and space science. The NASA Scientific and Technical Information (STI) program plays a key part in helping NASA maintain this important role.

The NASA STI Program operates under the auspices of the Agency Chief Information Officer. It collects, organizes, provides for archiving, and disseminates NASA's STI. The NASA STI program provides access to the NASA Aeronautics and Space Database and its public interface, the NASA Technical Reports Server, thus providing one of the largest collections of aeronautical and space science STI in the world. Results are published in both non-NASA channels and by NASA in the NASA STI Report Series, which includes the following report types:

- TECHNICAL PUBLICATION. Reports of completed research or a major significant phase of research that present the results of NASA programs and include extensive data or theoretical analysis. Includes compilations of significant scientific and technical data and information deemed to be of continuing reference value. NASA counterpart of peer-reviewed formal professional papers but has less stringent limitations on manuscript length and extent of graphic presentations.

- TECHNICAL MEMORANDUM. Scientific and technical findings that are preliminary or of specialized interest, e.g., quick release reports, working papers, and bibliographies that contain minimal annotation. Does not contain extensive analysis.

- CONTRACTOR REPORT. Scientific and technical findings by NASA-sponsored contractors and grantees.

- CONFERENCE PUBLICATION. Collected papers from scientific and technical conferences, symposia, seminars, or other meetings sponsored or cosponsored by NASA.

- SPECIAL PUBLICATION. Scientific, technical, or historical information from NASA programs, projects, and missions, often concerned with subjects having substantial public interest.

- TECHNICAL TRANSLATION. English-language translations of foreign scientific and technical material pertinent to NASA's mission.

Specialized services also include creating custom thesauri, building customized databases, organizing and publishing research results.

For more information about the NASA STI program, see the following:

- Access the NASA STI program home page at *http://www.sti.nasa.gov*

- E-mail your question via the Internet to *help@sti.nasa.gov*

- Fax your question to the NASA STI Help Desk at 301–621–0134

- Telephone the NASA STI Help Desk at 301–621–0390

- Write to:
  NASA Center for AeroSpace Information (CASI)
  7115 Standard Drive
  Hanover, MD 21076–1320

NASA/TM—2008-215492

The Effect of Simulated Lunar Dust on the Absorptivity, Emissivity, and Operating Temperature on AZ–93 and Ag/FEP Thermal Control Surfaces

James R. Gaier and John Siamidis
Glenn Research Center, Cleveland, Ohio

Scott R. Panko
Arctic Slope Research Corporation, Cleveland, Ohio

Kerry J. Rogers
Manchester College, North Manchester, Indiana

Elizabeth M.G. Larkin
Case Western Reserve University, Cleveland, Ohio

National Aeronautics and
Space Administration

Glenn Research Center
Cleveland, Ohio 44135

December 2008

Acknowledgments

This work is the result of a great deal of effort by a sizable team of dedicated professionals from many organizations. In addition to the authors and co-authors, Edward A. Sechkar (Arctic Slope Research Corporation) and Frank P. Lam (TFOME) provided engineering and technical support of the LDAB facility. Donald A. Jaworske (NASA GRC) oversaw the fabrication of the test samples and acted as a general resource on the behavior of thermal control coatings. Mark J. Hyatt (NASA GRC) and Ryan Stephan (NASA JSC) provided continued program guidance. KJR wishes to thank the Lewis Educational Research and Collaboration Internship Program for their support.

Level of Review: This material has been technically reviewed by technical management.

Available from

NASA Center for Aerospace Information
7115 Standard Drive
Hanover, MD 21076–1320

National Technical Information Service
5285 Port Royal Road
Springfield, VA 22161

Available electronically at http://gltrs.grc.nasa.gov

The Effect of Simulated Lunar Dust on the Absorptivity, Emissivity, and Operating Temperature on AZ–93 and Ag/FEP Thermal Control Surfaces

James R. Gaier and John Siamidis
NASA Glenn Research Center
Cleveland, Ohio 44135

Scott R. Panko
Arctic Slope Research Corporation
Cleveland, Ohio 44135

Kerry J. Rogers
Manchester College
North Manchester, Indiana 46962

Elizabeth M.G. Larkin
Case Western Reserve University
Cleveland, Ohio 44106

Abstract

JSC–1AF lunar simulant has been applied to AZ–93 and AgFEP thermal control surfaces on aluminum or composite substrates in a simulated lunar environment. The temperature of these surfaces was monitored as they were heated with a solar simulator and cooled in a 30 K coldbox. Thermal modeling was used to determine the absorptivity (α) and emissivity (ε) of the thermal control surfaces in both their clean and dusted states. Then, a known amount of power was applied to the samples while in the coldbox and the steady state temperatures measured. It was found that even a submonolayer of simulated lunar dust can significantly degrade the performance of both white paint and second-surface mirror type thermal control surfaces under these conditions. Contrary to earlier studies, dust was found to affect ε as well as α. Dust lowered the emissivity by as much as 16 percent in the case of AZ–93, and raised it by as much as 11 percent in the case of AgFEP. The degradation of thermal control surface by dust as measured by α/ε rose linearly regardless of the thermal control coating or substrate, and extrapolated to degradation by a factor 3 at full coverage by dust. Submonolayer coatings of dust were found to not significantly change the steady state temperature at which a shadowed thermal control surface will radiate.

Introduction

During the highly successful Apollo program to land humans on the moon and return them safely to earth, lunar surface operations were hampered by the effects of a fine, pervasive, highly adhesive dust. The mission records contain references to challenges involving obscuration of vision, clogging of equipment, coating of surfaces, abrasion of surfaces, degradation of seal performance, degradation of thermal performance, and minor health issues (ref. 1). Some of the potentially most serious consequences were due to lunar dust on thermal control surfaces, which caused overheating in several of the science experiments and the batteries of the lunar roving vehicle (ref. 2).

The Vision for Exploration, announced in 2004, has since been formalized by Congressional legislation as the revised the United States Space Policy. It calls for a return to the moon by 2020. The current architecture calls for the establishment of a lunar outpost within the first few years which will be inhabited for tours of duty as long as 6 months. Infrastructure such as power system and lunar rovers will be expected to have even longer service lives so they can be used by successive crews. Given the extent of the problems caused by dust during the Apollo program, in which the astronauts spent no more than three days on the surface and none of the equipment was reused, it is only prudent to try to better understand and mitigate the risk posed by the dust. The Exploration Technology Development Program (ETDP) was chartered to develop enabling and enhancing technologies required by Constellation systems to allow sustainable, affordable human exploration missions. Within ETDP, both the Dust Mitigation Project and the Advanced Thermal Control Project have recognized the importance of this problem, and have developed joint tasks to address it. This study compiles the results of the first year of these joint tasks. The objective of the research was to quantify the effects that a sub-monolayer of lunar dust may be expected to have on thermal control surfaces. It is thought that thick dust layers will be relatively easy to remove from thermal control surfaces by techniques such as brushing, blowing off with a gas jet, or electrostatic removal. It is anticipated, though, that those techniques will not be completely effective and there is a question as to what quantity of dust needs to be removed. A second, implied, objective is to establish test protocols for the exposure and characterization of the test samples so that the

effectiveness of dust mitigation strategies can be quantified. This will be critical for cost-benefit analyses and trade studies.

Methods and Materials

Data Collection

The first series of tests utilized a white thermal control paint (AZ–93) and a second surface mirror (Ag coated FEP Teflon (Dupont)) as the thermal control surfaces. The thermal control surfaces were applied either to 2.54 cm (1 in.) diameter aluminum substrates, or to identically fabricated composite samples. The composites, which were fabricated in-house, contained a surface layer of K-1100 high thermal conductivity graphite fibers and enough layers of PAN-based structural carbon fibers to give a thickness of 6.4 mm (0.25 in.) in a matrix of RS-3 isocyanate resin. This is the same composite structure used by the thermal control group for composite radiators within the ETDP's Fission Surface Power project. The laminate was laid up as a single sheet and then the round disks were machined from that sheet. The AZ–93 paint was applied by AZ Technology (Huntsville, Alabama). The AgFEP samples were fabricated by Sheldahl (Northfield, Minnesota) from 12.7 μm (5 mil) thick FEP Teflon which was coated with a few tens of nm of silver and a few tens of nm of Inconel as a sealing layer to prevent oxidation. They were hand-applied to the samples using adhesive.

The tests were carried out using the NASA lunar dust adhesion bell jar (LDAB). The lunar simulation facility enables the simulated lunar dust to be heated, dried, plasma-cleaned, chemically reduced, and sieved into samples *in situ*. It operates at a pressure of 10^{-7} to 10^{-8} Torr. The sample, pristine or dusted, can be heated using a 20-sun xenon arc lamp solar simulator, and radiatively cooled in a 30 K cold-box. Details of the LDAB are available elsewhere (ref. 3). Figure 1(a) shows a photograph of one of the AZ–93 painted composite samples. As with the previous tests, two samples of the same material were exposed during each test in a single sample holder. Figure 1(b) shows two samples mounted in the LDAB sample holder.

One sample was used in the dynamic test where the sample was heated using an unfiltered xenon arc lamp, and then cooled by sliding into a cold box, which is lined with an absorbing material (Vel-Black) and maintained at about 30 K with a recycling helium refrigerator. The second sample was used in the steady state tests and was identical to the first except that a 10 Ω resistance heater was bolted to the underside of the sample. The sample was translated into the cold box and allowed to cool to equilibrium. Then 0.250 W of electrical power was supplied to the heater and the sample allowed to come to its new equilibrium temperature. Subsequently, 1.00 W of electrical power was applied and the sample again allowed to come to its new equilibrium temperature. To minimize heat losses, the samples were supported at their edges by three layers of 0.25 mm (10 mil) thick Kapton (Dupont). Temperatures were monitored throughout the test with thermocouples made with 36 AWG wire embedded into the back of the substrate.

Lunar Simulant Processing

The lunar dust simulant chosen for these tests was JSC–1AF. The "F" in the label indicates that it is enriched in the fine fraction. About half of the particles are 20 μm or smaller. This is the baseline lunar simulant that is being used most widely by NASA and most of the community. In bulk chemistry, it closely resembles soils of the Mare that were returned during Apollo 14. It was selected, not because it is the best simulant available, but because at this time it is the *de facto* NASA standard.

The lunar simulant was degassed in vacuum at high temperature (> 200 °C) overnight with intermittent stirring. It was cleaned using an air plasma for 1 hr to oxidize organic contaminants from its surface. It was then subjected to a 4 percent hydrogen in helium plasma for 1 hr to chemically reduce the surface and implant some amount of hydrogen into the dust grains, to simulate the implanted solar wind on the lunar surface. The dust was applied to the samples through either a 25 or a 32 μm sieve so that only the dust fraction would be applied. Sub-monolayer coatings of dust were applied in all cases for these tests.

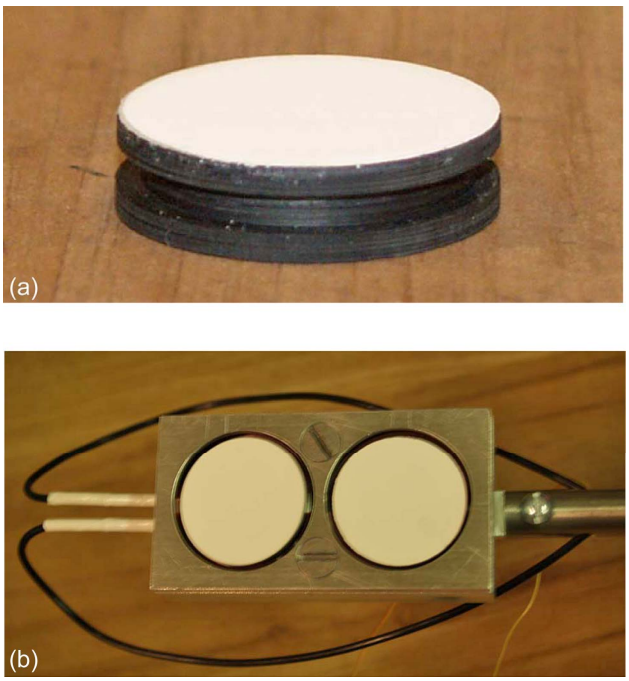

Figure 1.—(a) Composite sample coated with AZ-93, (b) two 2.54 cm diameter samples of AZ-93 coated aluminum in the sample holder. The black wires supply the electrical power to the left sample for the steady state test. The thin yellow wires in the photo are two thermocouples, one connected to each sample.

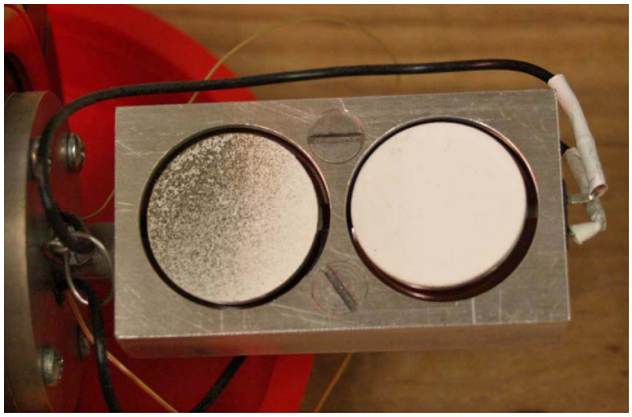

Figure 2.—Photograph of the two AZ93AI-1 samples that were dusted at the same time in the configuration shown. The left hand sample, particularly on its left half, was coated much more heavily than the right hand sample.

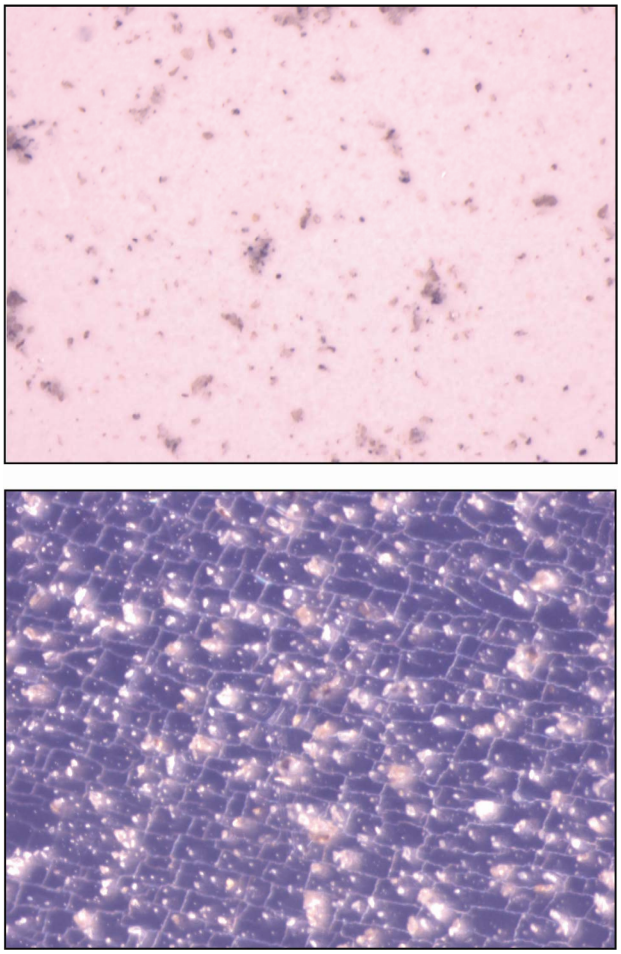

Figure 3.—Examples of photomicrographs of the AZ93 sample (left) and AgFEP sample (right) that were used in the analysis of fractional dust coverage. The area covered in each photomicrograph is about 1 mm^2.

Dust Coverage Characterization

It proved surprisingly difficult to apply an even coating of dust on thermal control surface samples. It was thought that a simple sinusoidal motion of the sieve would deposit evenly and reproducibly. This has proven not to be the case. Varieties of jarring and vibrating motions were also employed, but did not give consistently even coatings. To complicate the problem further, the dust that had been treated *in vacuo* it behaved differently than it did in the tests that were conducted in air. Schemes that would work on one run would not work on the next. Time that the dust was sifted onto the sample correlated very poorly with the amount of dust deposited. That is, more dust may be deposited in a 60 sec run than on a 600 sec run. Typical results are shown in figure 2. It can be readily seen that the left sample has much more dust deposited on it than the right sample.

The characterization of fractional coverage by dust is complicated by the fact that all particles deposited on the samples are smaller than 32 μm, because of the sieve. Thus, although the right hand sample in figure 2 appears to be clean, microscopic investigation reveals that about 5 percent of its surface is covered with dust, and indeed its absorptance is increased.

Determining the fractional occultation of the thermal control surface by a sub-monolayer of sub-25 μm particles is not straightforward. The sample disks have an area of 5×10^8 μm^2, and the largest particles an area of 500 μm^2. In order to count such small particles, magnification of at least 100× is required. At 100× the area imaged by our microscope is 968×726 μm, so there are 641 non-overlapping frames needed to completely cover the surface of the sample disk. Frames that were partially filled with the sample image were ignored. This is permissible because the pattern of the dust distribution is larger than the sample, so we are in a sense only sampling already from a larger distribution. Rather than count the particles in all 641 frames for each of 17 samples it was decided to analyze a statistically significant random sample of the frames.

In order to take rigorously random samples, a computer controlled *x*-*y*-θ stage was installed on the microscope. Each sample was mounted on the stage with a specific orientation (i.e., the thermocouple holes aligned in the θ = 0 direction). The random number generator in Microsoft Excel (Microsoft Corporation) was used to set the θ value for each sample in order to account for systematic angular consistencies that might be present in the dust distribution pattern. The percentage of dust coverage on each sample was estimated by superimposing a grid onto each sample dividing the sample into 641 non-overlapping frames of equal size. Frames on each sample were then randomly chosen using the random number generator and each selected field was located and digitally photographed. The dust appeared dark on the AZ–93 coating, but light on the AgFEP coatings, as can be seen in figure 3. Because of the sieving, all particles were less than 25 μm in size. Image-Pro (Cullimore & Ring Technologies) software was used to determine the proportion of black (128 to 256 on the grey scale) to white pixels (0 to 128 on the grey

scale) in each photograph. The percentage of black pixels represents the overall dust coverage of the tested field on AZ–93, and the percentage of white pixels represents the overall dust coverage of the tested field on AgFEP. A 95 percent confidence interval (*CI*) was also calculated around each mean to determine the precision of this estimated mean $(\overline{n})$ using equation (1):

$$CI = \overline{n} \pm z\sqrt{\frac{p(1-p)}{n-1}\left(1-\frac{n}{N}\right)} \qquad (1)$$

where z is the critical value from the normal distribution (1.96 for a 95 percent *CI*), p is the sample proportion (percentage of pixels occulted by dust), n is the sample size (number of frames examined), and N is the population size (total number of frames in a sample).

The mean, standard deviation, and confidence interval as a function of frames examined for a typical sample are plotted in figure 4. It can be seen that the 95 percent confidence interval begins to flatten out, at about 50 frames, so measuring beyond that number would yield limited returns. Thus, 50 frames were measured for each sample.

Absorptivity and Emissivity Characterization

The thermal modeling was performed using Thermal Desktop (Cullimore & Ring Technologies), a PC based design environment for generating thermal models of electronics and vehicles. Thermal Desktop incorporates both parameter based finite difference surfaces with finite elements and CAD technology to model thermal problems. Thermal Desktop develops the capacitance and conductance network for input to SINDA/Fluint which is a comprehensive finite-difference, lumped parameter (circuit or network analogy) tool for heat transfer design analysis and fluid flow analysis for complex systems. Thermal Desktop 5.1 Patch 3 was used to generate the thermal model, which consists of 743 nodes and 1840 linear conductors. A visualization of the model and the material parameters used in it are shown in figure 5.

For the pristine samples during heating, the optical properties (α/ε) of the coated sample are set to its initial values. Subsequently, the power of the heating lamp was varied to match the temperature of the test run. Once the power of the lamp was established, the absorptivity (α) was varied for each test run until there was less that one percent difference in the weighted average temperatures between each test run and each analysis run. During cooling, the emissivity (ε) was varied for each test run until there was less than one percent difference in the weighted average temperatures between each test run and each analysis run.

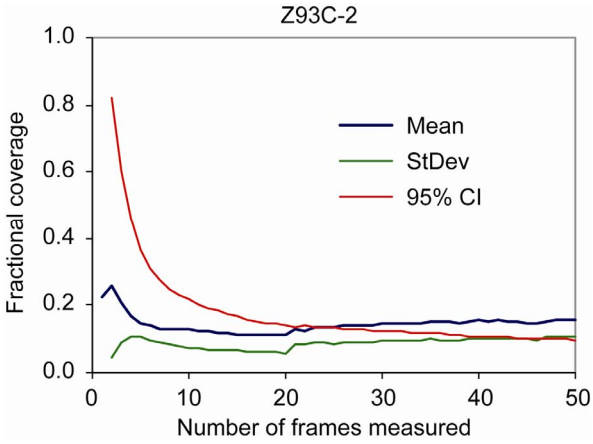

Figure 4.—Statistical parameters as a function of frames examined for dusted sample.

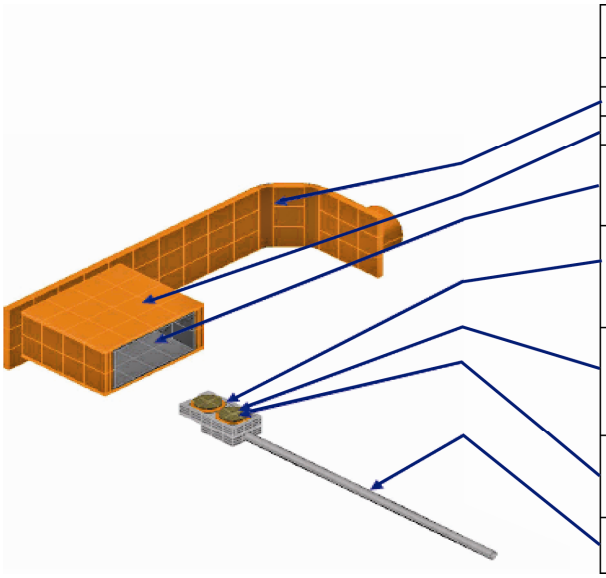

	Material	Material cond., W/mK	Material cp., J/KgK	Material finish	Material finish α/ε
Chamber	SS 316	16.3	504	SS polished	0.42/0.11
Blend copper	Copper	406.4	380	Buffed copper	0.30/0.03
Copper box	Copper	406.4	380	Buffed copper	0.30/0.03
Vel-black layer inside copper box	Carbon fiber	360	628	Black paint	0.95/0.95
Sample holder	AL 6061-T8	f(T) = 43.3 at 32 K to 175.6 at 743.9K	f(T) = 64.6 at 34.6 K to 1126.8 at 810.9K	Al polished	0.15/0.05
Aluminum sample	AL 6061-T8	f(T) = 43.3 at 32 K to 175.6 at 743.9K	f(T) = 64.6 at 34.6 K to 1126.8 at 810.9K	Z-93	Initial 0.20/0.91 then varied
Composite sample	3 layer composite	Varies by layer 1st layer; 1100 2nd and 3rd; 5	~1000	AgFEP	Initial 0.08/0.81 then varied
Sample holder rod	SS 304	16.3	500	SS machined	0.47/0.14

Figure 5.—Picture of the thermal model and parameters used in its construction.

For the dusted samples during heating, and for the same lamp power established previously, the α was varied for each test run until there was less than one percent difference in the weighted average temperatures between each test run and each analysis run. During cooling, the ε was varied for each test run until there was less that one percent difference in the weighted average temperatures between each test run and each analysis run.

Results and Discussion

Dynamic Test Results on Pristine Samples

In order to determine the quality of data generated by the LDAB two sets of dynamic test measurements were made on pristine AZ–93 without disturbing the sample in between. The heating and cooling curves are shown in figure 6. They show the instrument reproducibility of the LDAB calorimetry system.

There were also two tests where a sample was measured, removed from the LDAB, and remeasured at a later time. This introduces additional variabilities regarding the exact positioning and orientation of the sample with respect to the heating lamp. Figure 7 shows the heating and cooling curves for AgFEPAl-1, which was re-measured twice. The bright red line (slightly lower) on the heating curve was measured before physical marking of the rod translation position for measurement. That the reproducibility was improved by this is shown by the close correlation of the other two lines. The sample rotational orientation is maintained by the use of a spirit level attached to the sample holder support rod. However, some rotational misorientation can still occur because the Kapton sample mount is thin to keep down thermal losses, and so also somewhat flexible.

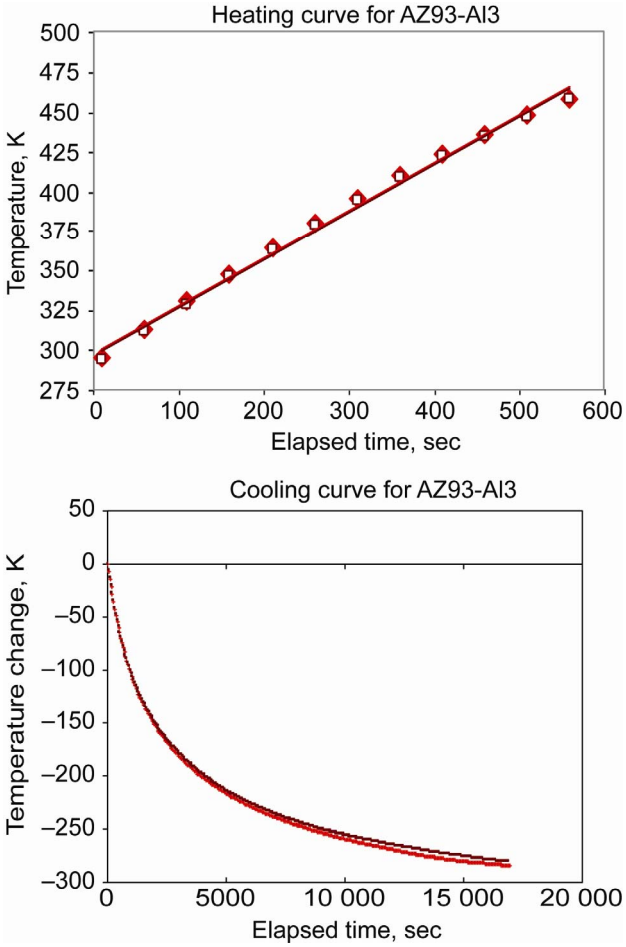

Figure 6.—Heating curve and cooling curve for sample Z93Al-3 taken two different days (light red ♦ and dark red □) shows that the reproducibility of the data produced in the LDAB is high.

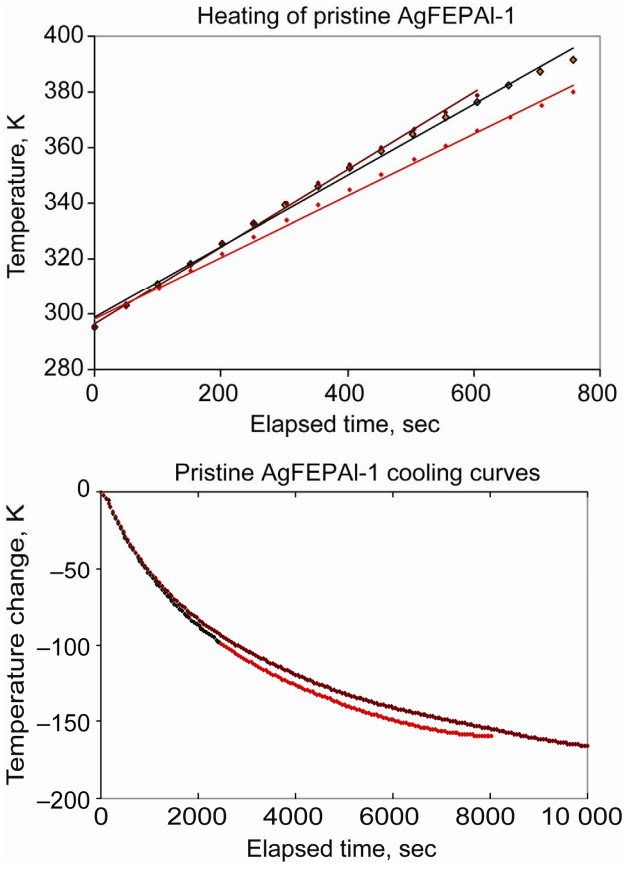

Figure 7.—Heating curves and cooling curves for sample AgFEPAl-1 taken on three different days with the samples being removed in between and repositioned show that the reproducibility of the data is sensitive to the exact position and orientation.

AZ–93 Painted Aluminum

Figure 8 shows the temperature data for the heating and cooling curves for the five different pristine AZ–93 painted aluminum samples as discrete points. The fit from the thermal model for each run is shown as a line in the same color. As can be seen in figure 8 and table I, the reproducibility of the experiment was quite good. The α of the coating was found to be 0.173 ± 0.029, and the ε was 0.886 ± 0.024. The α model fit the data within 0.03 percent in all five cases, and the ε model within 1.67 percent. It should be pointed out that variations in lamp intensity, translational and rotational sample positioning, and temperature dependence of thermal properties are all contained in the measurements of α and ε. Nevertheless, the values determined for α and ε are well within the literature values for AZ–93 and similar white thermal control paints.

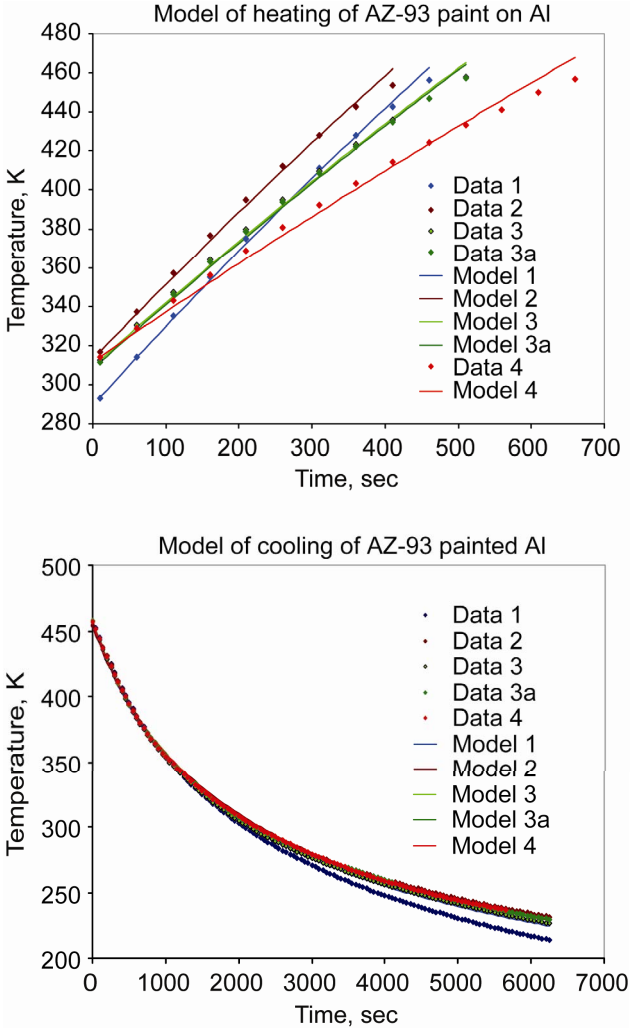

Figure 8.—The model fit for the heating and cooling curves for the five pristine AZ-93 on aluminum substrate data sets.

Dynamic Test Results on Dusted Samples

Dusted AZ–93 Painted Aluminum

Figure 9 shows the temperature data for the heating and cooling curves for the five different dusted AZ–93 painted aluminum samples as discrete points. The fit from the thermal model for each run is shown as a line in the same color. For clarity the colors used and order reported in the legend of samples in figure 9 corresponds to the samples in figure 8, (i.e., Sample 1 was 50 percent covered with dust.) Note that Samples 3 and 3a in figure 8 are the same sample, evaluated twice, and that the sample 49 percent covered with dust is best considered the continuation of Sample 3a. The percent of the surface covered with dust is reported in table I. The model fit the α data to 0.05 percent or better. Note that the more heavily a sample is covered with dust, the steeper the slope in the time-temperature plot, hence the higher the α. This is what would be expected by putting dark dust on a white paint. The model fit the ε data to 0.42 percent or better.

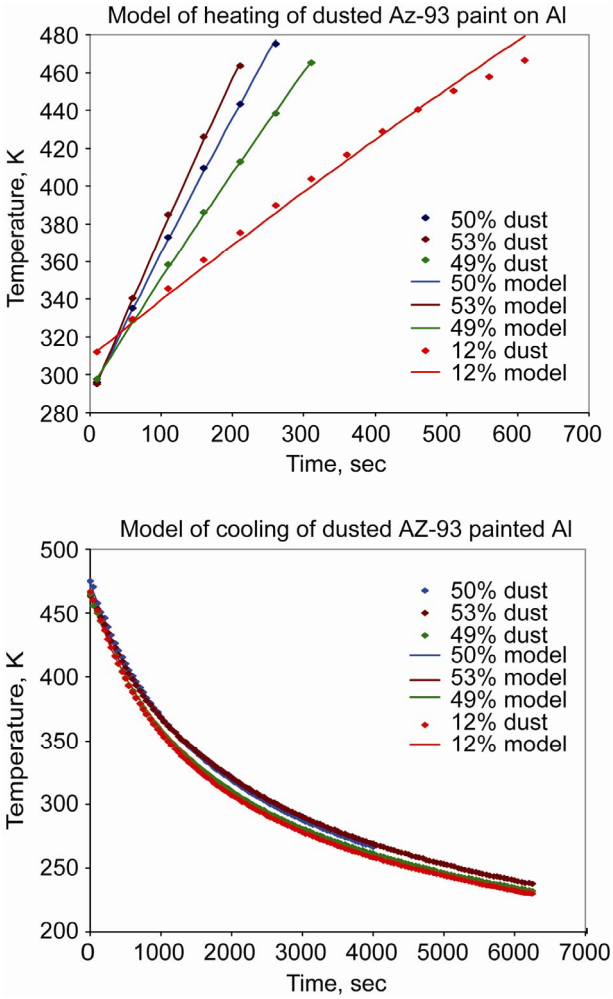

Figure 9.—The model fit for the heating and cooling curves for the four dusted AZ-93 on aluminum substrate data sets.

TABLE I.—BEST FIT PARAMETERS FROM THE MODEL OF THE AZ PAINTED ALUMINUM SAMPLES.

Z93 on AL	Sample 1	Sample 2	Sample 3	Sample 3a	Sample 4	AVE.
Pristine α (heating)	0.201	0.196	0.166	0.166	0.130	**0.173**
Weighted average difference between data and model temperatures	–0.01%	–0.02%	0.01%	0.03%	0.01%	**0.00%**
Pristine ε (cooling)	0.920	0.855	0.895	0.895	0.875	**0.886**
Weighted average difference between test and analysis temperatures	–1.67%	0.00%	–0.42%	0.44%	0.02%	**–0.33%**
Dust coverage	50.2%	52.7%	-------	49.9%	12.5%	-------
Dusted α (heating)	0.390	0.447	-------	0.297	0.153	-------
Weighted average difference between data and model temperatures	–0.03%	0.01%	-------	0.03%	–0.05%	-------
Dusted ε (cooling)	0.800	0.750	-------	0.862	0.880	-------
Weighted average difference between data and model temperatures	0.10%	0.17%	-------	–0.01%	–0.42%	-------
$\alpha_{(dusted)}/\alpha_{(pristine)}$	**1.94**	**2.28**	-------	**1.79**	**1.18**	-------
$\varepsilon_{(dusted)}/\varepsilon_{(pristine)}$	**0.87**	**0.88**	-------	**0.96**	**1.01**	-------

At this point a comparison can be made between the measured absorptance and that which might be expected. A reasonable model to use is the rule of mixtures model which states that there are no interactions between the dust particles and the thermal control surface. Thus, if a surface is one quarter covered with dust, the absorptance of that one quarter should have the absorptance of bulk dust, and the absorptance of the remaining three quarters of the surface should be unaffected. The definition of relative absorptance can be written in terms of the rule of mixtures as equation (2).

$$\alpha_{\text{rel}} = \frac{\left(f_{\text{dust}}\alpha_{\text{dust}} + f_{\text{bare}}\alpha_{TCM}\right)}{\alpha_{TCM}} \qquad (2)$$

where f_{dust} and f_{bare} are the fractions of the surface covered by dust and not covered by dust respectively, and must sum to 1.00. The α_{rel} is the relative absorptance, the α_{dust} is the absorptance of the dust, taken to be 0.76, and the α_{TCM} is the absorptance of the thermal control material which is taken to be 0.173 for AZ–93. Figure 10 shows the measured relative absorptance compared to the model for AZ–93.

The data fall considerably below the model line. The discrepancy appears too systematic for it to be a result of the perhaps rather large error in the fractional coverage measurements. It is possible that the absorptance is lower because the bulk value for the lunar regolith absorptance was used. As can be seen in figure 11, most of the individual grains of the JSC-1AF lunar simulant are transparent (being plagioclase). So perhaps part of the light that gets trapped in multiple layers of dust is simply transmitted through to the coating when it is sub-monolayer.

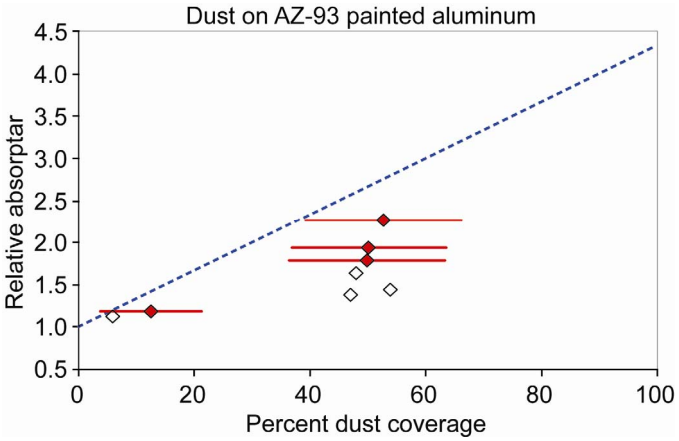

Figure 10.—Plot of $\alpha/\alpha_{\text{pristine}}$ as a function of fractional dust coverage for the AZ-93Al samples. The (♦) are mean percent for each experiment and the horizontal lines bound the coverage at the 95 percent confidence interval. The (✧) are the dust coverage estimates reported in the milestone 1 report, and the blue line is the rule of mixtures model.

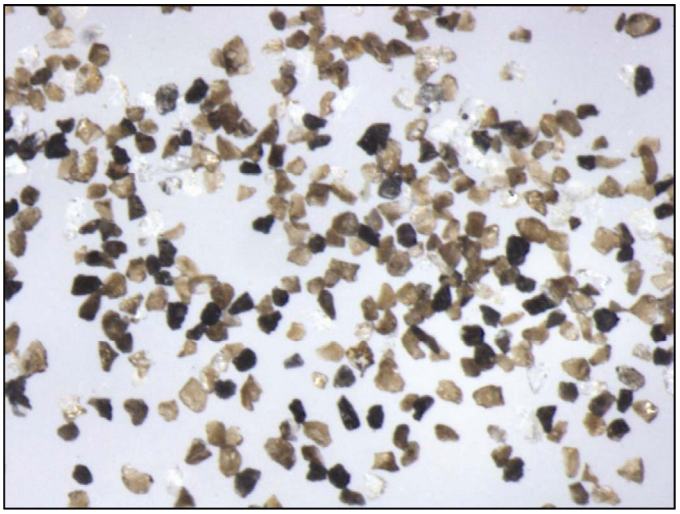

Figure 11.—Photomicrograph of JSC-1AF lunar simulant. Note that most of the particles are transparent.

AZ–93 Painted Composite

Figure 12 shows the temperature data for the heating and cooling curves for the four different pristine AZ–93 painted composite samples. The same convention is used where the data are represented as discrete points and the fit from the thermal model as a line in the same color. As can be seen in figure 12 and table II, the reproducibility of the experiment was also quite good. The α of the coating was found to be 0.196 ± 0.006, and the ε was 0.833 ± 0.026. The α model fit the data with 0.06 percent or less in all four cases, and the ε model within 0.28 percent. The values determined for α and ε are well within the literature values for AZ–93. In comparing α and ε of the same paint applied to the two different surfaces it is noted that the α is somewhat higher (13 percent) for the composite samples, and the ε is somewhat lower (6 percent lower). The higher α of the painted composite could be explained it the paint is not entirely opaque, since the alpha of the composite is much higher than that of the aluminum. The ε of the dust, 0.76 is somewhat lower than that of the coating.

Figure 13 shows the temperature data for the heating and cooling curves for the four different dusted AZ–93 painted composite samples. The percent of the surface covered with dust is reported in table II. The model fit the α data to 0.06 percent or better. The model fit the ε data to 0.28 percent or better.

Dusted AZ–93 Painted Composite

The comparison between the measured absorptance and that which might be expected using the rule of mixtures is shown in figure 14. Once again the data, even including the range represented by the 95 percent confidence interval, fall considerably below the model line. The relationship is similar to what was seen with the AZ–93 painted aluminum samples, as would be expected.

TABLE II.—BEST FIT PARAMETERS FROM THE MODEL OF THE AZ PAINTED COMPOSITE SAMPLES.

AZ–93 on Composite	Sample 1	Sample 2	Sample 3	Sample 4	AVE.
Pristine α (heating)	0.189	0.199	0.201	0.193	**0.196**
Weighted average difference between data and model temperatures	0.01%	–0.04%	–0.02%	–0.06%	**–0.03%**
Pristine ε (cooling)	0.81	0.85	0.86	0.81	**0.833**
Weighted average difference between test & analysis temperatures	–0.03%	–0.08%	0.18%	0.28%	**0.09%**
Dust coverage	23.9%	15.8%	54.4%	54.6%	--------
Dusted α (heating)	0.235	0.195	0.365	0.34	--------
Weighted average difference between data and model temperatures	0.15%	–0.09%	0.02%	0.03%	--------
Dusted ε (cooling)	0.86	0.82	0.72	0.8	--------
Weighted average difference between data and model temperatures	0.00%	–0.01%	0.03%	–0.28%	--------
$\alpha_{(dusted)}/\alpha_{(pristine)}$	**1.24**	**0.98**	**1.82**	**1.76**	--------
$\varepsilon_{(dusted)}/\varepsilon_{(pristine)}$	**1.06**	**0.96**	**0.84**	**0.99**	--------

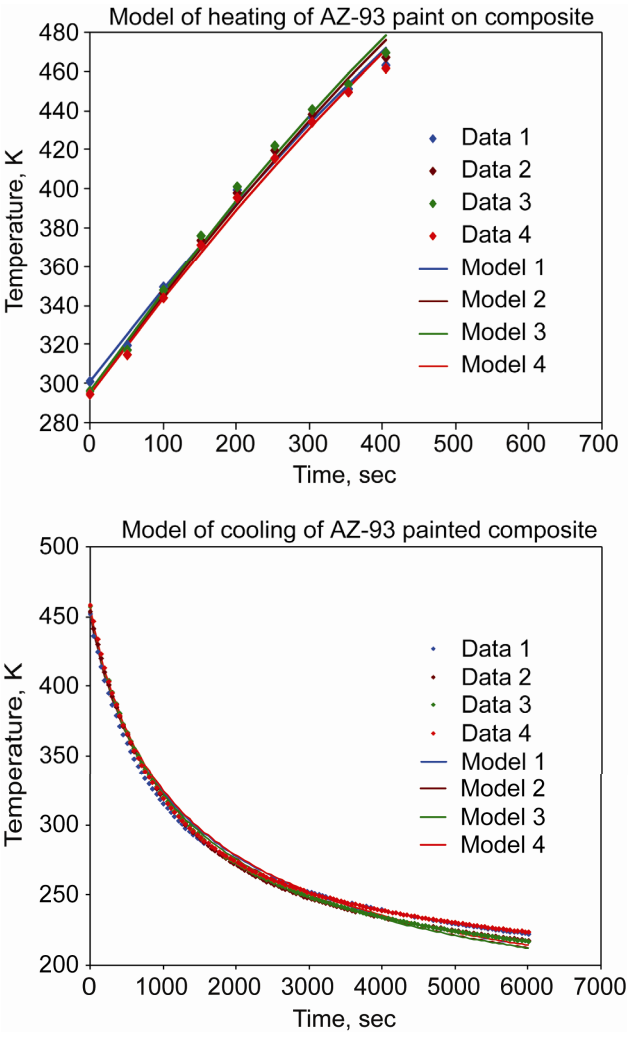

Figure 12.—The model fit for the heating and cooling curves for the five pristine AZ-93 on composite substrate data sets.

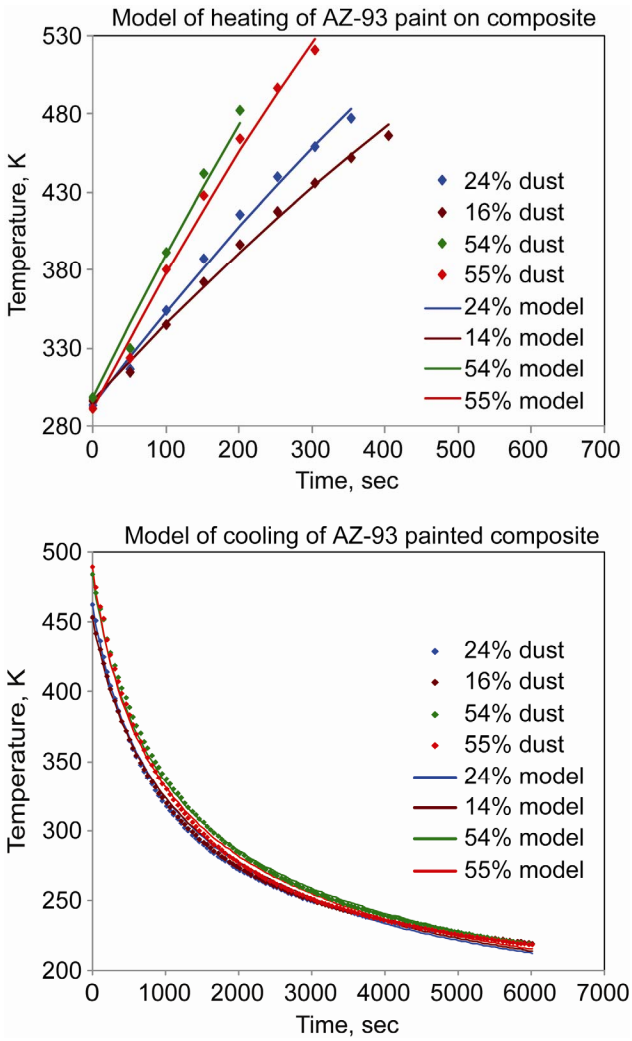

Figure 13.—The model fit for the heating and cooling curves for the four dusted AZ-93 on composite substrate data sets.

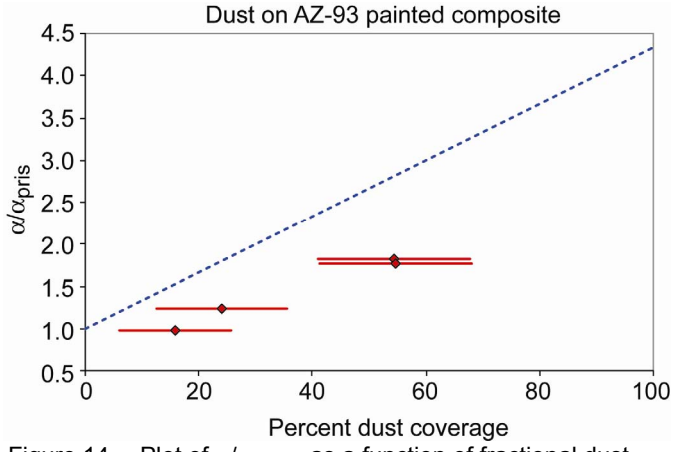

Figure 14.—Plot of $\alpha/\alpha_{pristine}$ as a function of fractional dust coverage for the AZ-93 composite samples. The (♦) are mean percent for each experiment and the horizontal lines bound the coverage at the 95 percent confidence interval.

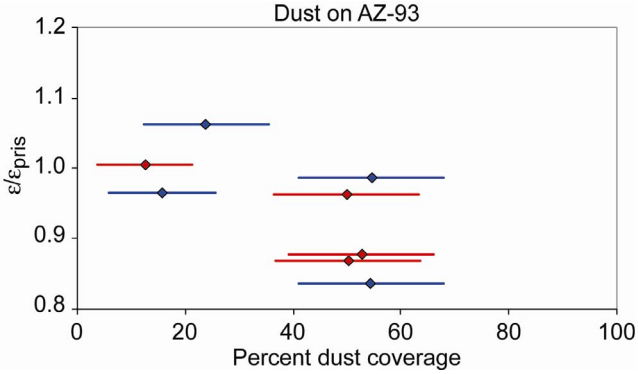

Figure 15.—Plot of $\varepsilon/\varepsilon_{pristine}$ as a function of fractional dust coverage for the AZ-93 painted on aluminum (red) and composite (blue) samples.

It has been thought that since the lunar regolith is so dark that dust on a thermal control surface will have no appreciable effect on the ε. The data plotted in figure 15 suggest that there may be a drop off in the emittance of AZ–93 as even less than a monolayer of dust accumulates on it. When fully covered, ε may well drop to a level that is less than 80 percent that of clean AZ–93, which may bring it below 0.70. This is significant degradation.

AgFEP on Aluminum

Figure 16 shows the heating and cooling curves for the seven different data sets of AgFEP adhered to aluminum substrates. As with the AZ–93 samples, figure 16 and table III indicate that the reproducibility of the experiment was quite good. The α of the coating was found to be 0.073 ± 0.006, and the ε was 0.719 ± 0.041. The α model fit the data with 0.10 percent or better in all seven cases, and the ε model within

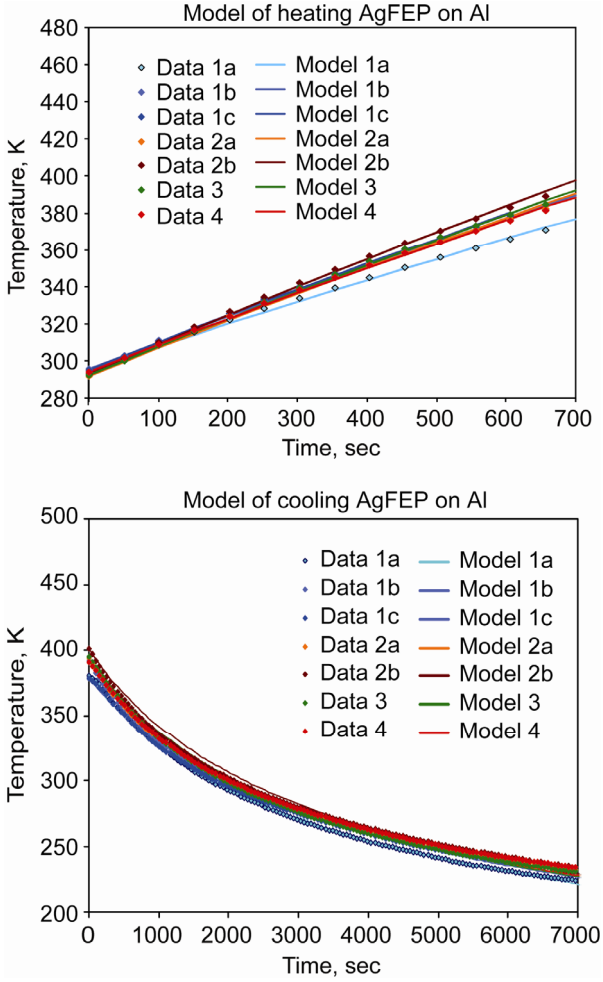

Figure 16.—The model fit for the heating and cooling curves for the seven pristine AgFEP on aluminum substrate data sets.

TABLE III.—BEST FIT PARAMETERS FROM THE MODEL OF THE AgFEP ON ALUMINUM SAMPLES.

AgFEP on AL	Sample 1a	Sample 1b	Sample 1c	Sample 2a	Sample 2b	Sample 3	Sample 4	AVE.
Pristine α (heating)	0.061	0.071	0.073	0.074	0.079	0.075	0.071	**0.073**
Weighted average difference between data and model temperatures	–0.05%	0.10%	–0.09%	–0.04%	0.05%	0.00%	0.06%	**0.00%**
Pristine ε (cooling)	0.770	0.800	0.700	0.700	0.700	0.720	0.700	**0.719**
Weighted average difference between test & analysis temperatures	–0.18%	0.27%	–0.26%	0.06%	0.02%	0.26%	–0.46%	**–0.04%**
Dust coverage	--------	--------	12.7%	--------	21.0%	47.6%	12.7%	--------
Dusted α (heating)	--------	--------	0.111	--------	0.121	0.280	0.090	--------
Weighted average difference between data and model temperatures	--------	--------	–0.30%	--------	–0.23%	–0.10%	–0.03%	--------
Dusted ε (cooling)	--------	--------	0.720	--------	0.780	0.730	0.720	--------
Weighted average difference between data and model temperatures	--------	--------	0.14%	--------	0.71%	0.33%	0.14%	--------
$\alpha_{(dusted)}/\alpha_{(pristine)}$	--------	--------	**1.52**	--------	1.64	3.73	1.27	--------
$\varepsilon_{(dusted)}/\varepsilon_{(pristine)}$	--------	--------	**1.03**	--------	1.11	1.01	1.03	--------

0.46 percent. The values determined for α and ε are well within the literature values for AgFEP. The analysis used in the Milestone 1 report found α to be 0.080 ± 0.007, and ε to be 0.807 ± 0.059. Though the values of α and ε found in this study were not radically different, they were both lower.

Dusted AgFEP on Aluminum

Figure 17 shows the temperature data for the heating and cooling curves for the four different dusted AgFEP on Al samples. The percent of the surface covered with dust is reported in table III. The model fit the α data to 0.30 percent or better. As with the AZ–93 samples, the α increased as more dust was added. The model fit the ε data to 0.71 percent or better.

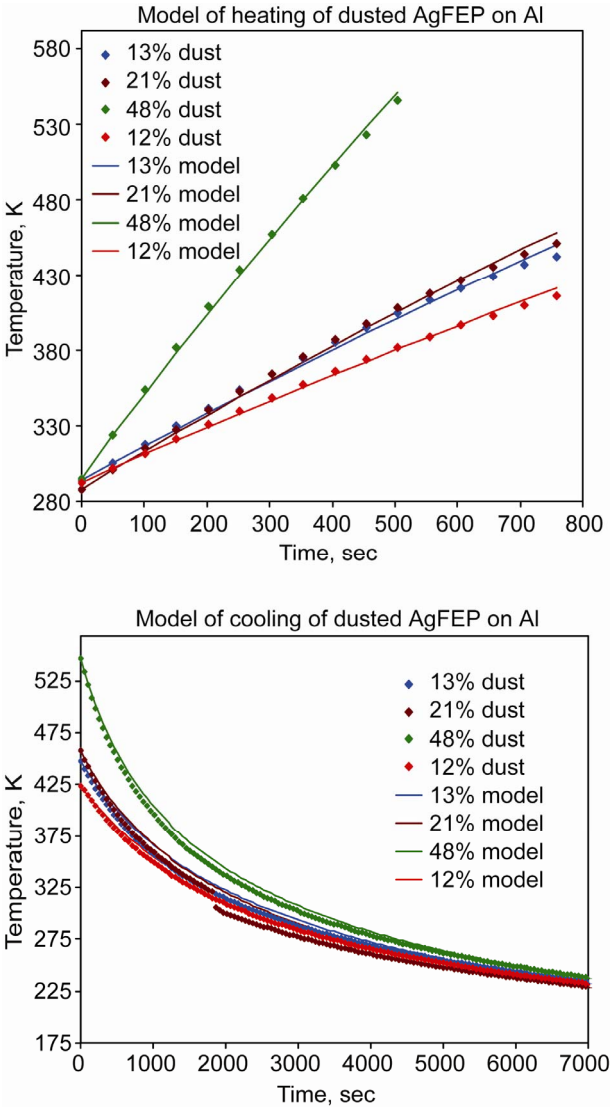

Figure 17.—The model fit for the heating and cooling curves for the four dusted AgFEP on aluminum substrate data sets.

The comparison between the measured absorptance increases due to dust deposition and those which might be expected using the rule of mixtures is shown in figure 18. Once again the data, even including the range represented by the 95 percent confidence interval, fall considerably below the model line. Even though the effect of dust on AgFEP is predicted to be more severe than on AZ–93 samples, the relationship between the rule of mixtures model and the measured data is similar.

AgFEP on Composite

Figure 19 shows the temperature data for the heating and cooling curves for the five different pristine AgFEP on composite samples. The same convention is used where the data are represented as discrete points and the fit from the thermal model as a line in the same color. As can be seen in figure 19 and table IV, the reproducibility of the experiment was not quite as good as the other experiments. This can be seen in the spread of the heating data in figure 19, which is much greater than the comparable AZ–93 data in figure 12. The α of the coating was found to be 0.101 ± 0.025, and the ε was 0.648 ± 0.038. In spite of this spread the α model fit the data within 0.09 percent or better in all four cases, and the ε model within 1.31 percent. The values determined for α are high and for ε are low compared to the literature values for AgFEP.

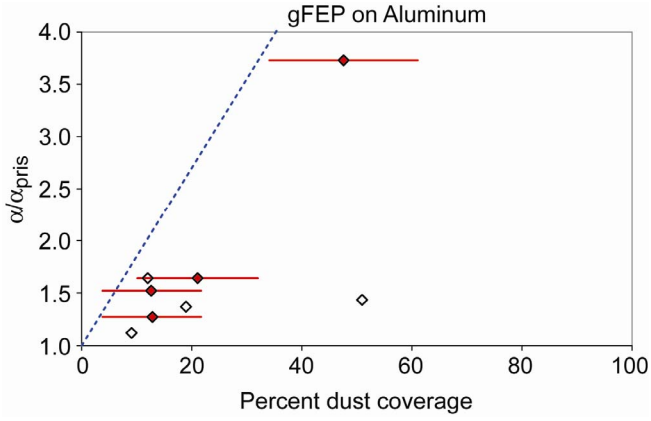

Figure 18.—Plot of $\alpha/\alpha_{pristine}$ as a function of fractional dust coverage for the AgFEP on aluminum samples. The (♦) are mean percent for each experiment and the horizontal lines bound the coverage at the 95 percent confidence interval. The (✧) are the dust coverage estimates reported in the Milestone 1 report, and the blue line is the rule of mixtures model.

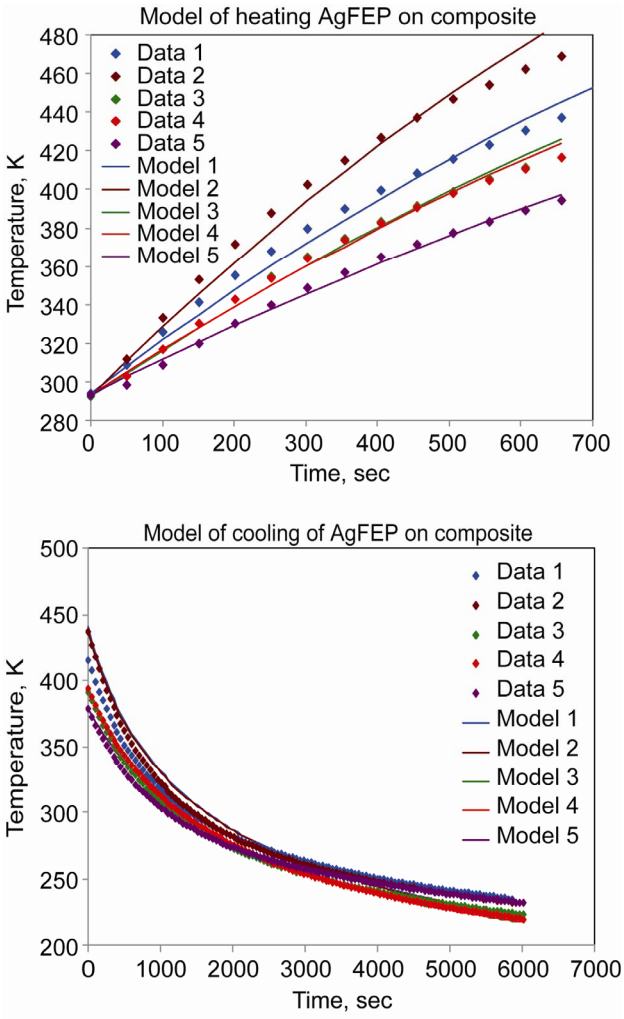

Figure 19.—The model fit for the heating and cooling curves for the seven pristine AgFEP on composite substrate data sets.

TABLE IV.—BEST FIT PARAMETERS FROM THE MODEL OF THE AgFEP ON COMPOSITE SAMPLES.

AgFEP on Composite	Sample 1	Sample 2	Sample 3	Sample 4	Sample 5	AVE.
Pristine α (heating)	0.108	0.141	0.094	0.092	0.072	**0.101**
Weighted average difference between data and model temperatures	0.04%	0.09%	–0.05%	–0.01%	0.07%	**0.03%**
Pristine ε (cooling)	0.620	0.620	0.690	0.690	0.620	**0.648**
Weighted average difference between test & analysis temperatures	1.31%	0.01%	0.02%	0.07%	0.66%	**0.35%**
Dust coverage	36.4%	5.0%	29.3%	39.2%	35.4%	--------
Dusted α (heating)	0.160	0.145	--------	0.197	0.130	--------
Weighted average difference between data and model temperatures	0.14%	–0.07%	--------	0.12%	0.06%	--------
Dusted ε (cooling)	0.690	0.625	--------	0.820	0.690	--------
Weighted average difference between data and model temperatures	–0.16%	0.15%	--------	–1.05%	0.19%	--------
$\alpha_{(dusted)}/\alpha_{(pristine)}$	**1.48**	**1.03**	--------	**2.14**	**1.81**	--------
$\varepsilon_{(dusted)}/\varepsilon_{(pristine)}$	**1.11**	**1.01**	--------	**1.19**	**1.11**	--------

Dusted AgFEP on Composite

Figure 20 shows the temperature data for the heating curves for the five different dusted AgFEP on composite samples, and four cooling curves. There was one less cooling curve to report because the thermocouple was pulled off of Sample 3 as it was being transferred from under the heating lamp to the cold box. In addition, there were problems with the composite out-gassing and the bubbles being trapped under the FEP causing it to pull away from the substrate in places. Not only does this affect the heat transfer properties between the FEP and the substrate, but it also made the dust coverage determination difficult because many of the frames were not flat enough for the microscope to focus on well. Since the dust coverage is determined optically, this provides an additional source of error in the dust coverage parameter. The percent of the surface covered with dust is reported in table IV. The model fit the α data to 0.14 percent or better. The large spread in pristine values of α means that the effect of dust on α is not as apparent in figure 20. For example, the pristine α of Sample 2 was higher than the dusted α of Sample 5, though the α of each sample increased. The model fit the ε data to 1.05 percent or better.

The comparison between the measured absorptance increases due to dust deposition and those which might be expected using the rule of mixtures is shown in figure 21. Once again the data, even including the range represented by the 95 percent confidence interval, fall considerably below the model line. The relationship between the rule of mixtures model and the measured data is similar to the other cases.

Given the effect of dust on the emittance of AZ–93 shown in figure 15, it is perhaps surprising that dust on AgFEP appears to have the opposite effect. Figure 22 shows that ε increases with dust coverage. When fully covered, ε may well rise to a level as high as 1.3 times greater than that of clean AgFEP, which may raise it above 0.90. This is a significant enhancement.

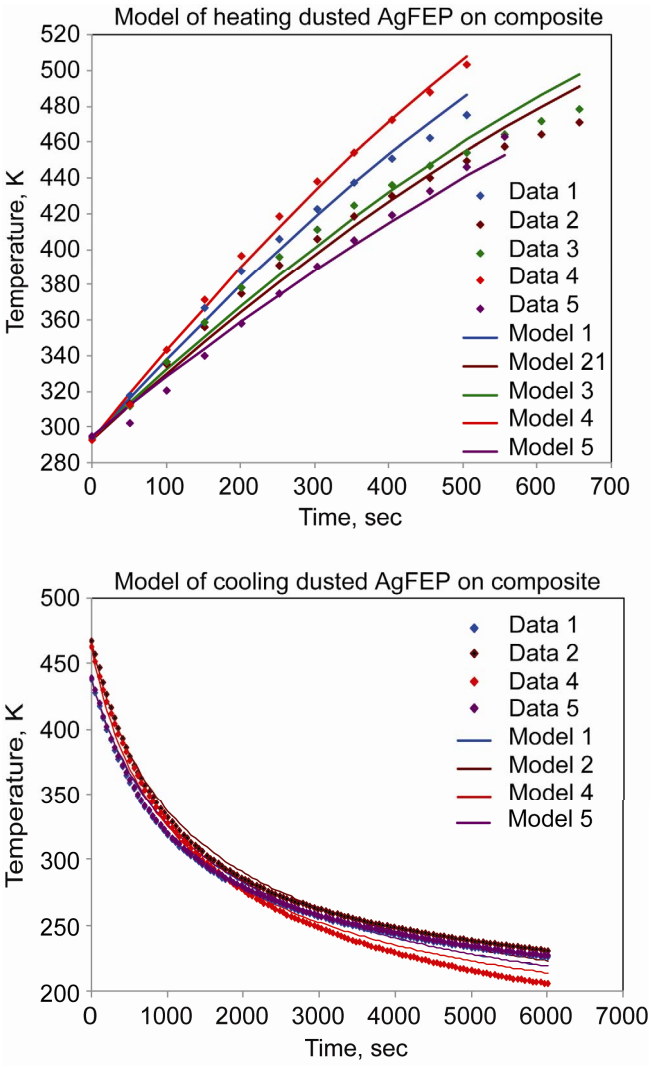

Figure 20.—The model fit for the heating and cooling curves for the four dusted AgFEP on composite substrate data sets.

Steady State Test Results

The steady state temperatures when 0.25 or 1.00 W is applied to the sample while setting in a 30 K coldbox are illustrated in figure 23. Two trends are apparent from these plots. First, it appears that the spread in the steady state temperatures of the pristine samples is as wide as the span of dust covered temperatures. This implies that a sub-monolayer level of dust coverage would not cause a shaded radiator to run hotter. Second, it appears that the AgFEP aluminum samples ran significantly (30 to 35 K) hotter than the other samples, and this is most evident when they had dust on them. The AgFEP composite radiator samples ran somewhat hotter than the AZ–93, particularly when clean. The AZ–93 on aluminum radiators ran the coolest.

To judge the overall thermal performance of a thermal control surface both the α and ε of the surface must be accounted for, generally as the ratio α/ε. Figure 24 is a plot of the total change in α/ε as a function of dust coverage for

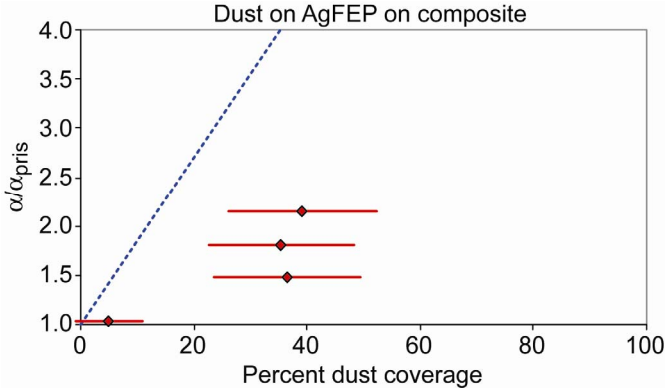

Figure 21.—Plot of $\alpha/\alpha_{pristine}$ as a function of fractional dust coverage for the AgFEP on composite samples. The (♦) are mean percent for each experiment and the horizontal lines bound the coverage at the 95 percent confidence interval.

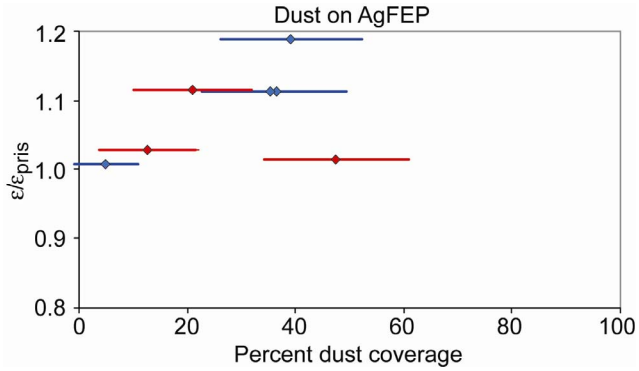

Figure 22.—Plot of $\varepsilon/\varepsilon_{pristine}$ as a function of fractional dust coverage for the AgFEP on aluminum (red) and composite (blue) substrates.

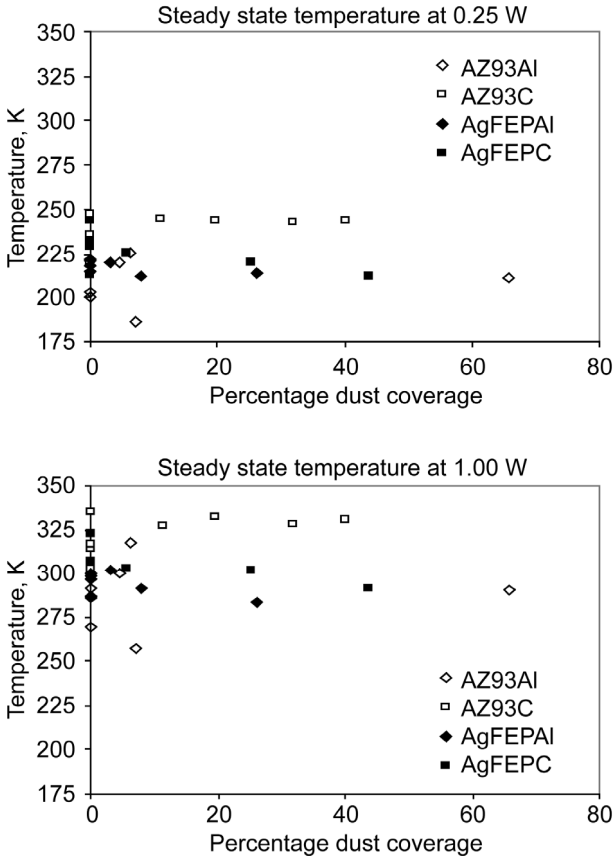

Figure 23.—The steady state temperatures of pristine and dusted samples radiating to a 30 K background with 0.25 and 1.00 W applied power.

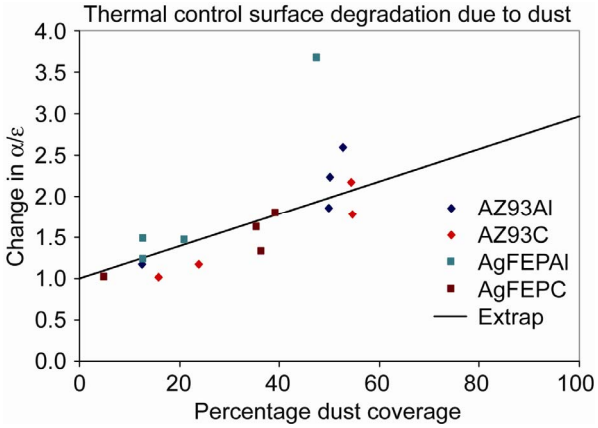

Figure 24.—The total change in α/ε as a function of dust coverage.

each of the four types of samples measured in this study. Interestingly, the α/ε values rose linearly with dust coverage regardless of the thermal control coating or substrate. A least squares line had an R^2 of 0.72, and extrapolated to degradation by a factor 3 for full coverage by dust.

Conclusions

There are three major conclusions that can be drawn from this study. The first is that even a sub-monolayer of simulated lunar dust can significantly degrade the performance of both white paint and second-surface mirror type radiators under simulated lunar conditions. As little as 12 percent dust coverage can degrade the α by as much as 50 percent.

The second conclusion is that the dust has an effect on the ε as well. It degrades it by as much as 16 percent in the case of 54 percent covered AZ–93, and improves it by as much as 11 percent in the case of 35 percent covered AgFEP. The degradation of thermal control surface by dust as measured by α/ε rose linearly regardless of the thermal control coating or substrate, and extrapolated to degradation by a factor 3 at full coverage by dust.

The third conclusion is that sub-monolayer coatings of dust do not significantly change the steady state temperature that a shadowed thermal control surface would operate at. This again emphasizes that although the ε is altered by the presence of a sub-monolayer of dust, the change in α is the major effect, and in the absence of incident radiation the dust has little effect on radiator performance.

References

1. J.R. Gaier, "The Effects of Lunar Dust on EVA Systems During the Apollo Missions," NASA/TM—2005-213610/REV1.
2. J.R. Gaier and D.A. Jaworske, "Lunar Dust on Heath Rejection System Surfaces: Problems and Prospects," STAIF07, Paper 26, and NASA/TM—2007-214814.
3. J.R. Gaier and E.A. Sechkar, "Lunar Simulation in the Lunar Dust Adhesion Bell Jar," Presented at the 45th AIAA Technical Conference as AIAA–2007–0963, and NASA/TM—2007-214704.

REPORT DOCUMENTATION PAGE	Form Approved OMB No. 0704-0188

1. REPORT DATE *(DD-MM-YYYY)*	2. REPORT TYPE	3. DATES COVERED *(From - To)*
01-12-2008	Technical Memorandum	

4. TITLE AND SUBTITLE
The Effect of Simulated Lunar Dust on the Absorptivity, Emissivity, and Operating Temperature on AZ-93 and Ag/FEP Thermal Control Surfaces

5a. CONTRACT NUMBER

5b. GRANT NUMBER

5c. PROGRAM ELEMENT NUMBER

6. AUTHOR(S)
Gaier, James, R.; Siamidis, John; Panko, Scott, R.; Rogers, Kerry, J.; Larkin, Elizabeth, M., G.

5d. PROJECT NUMBER

5e. TASK NUMBER

5f. WORK UNIT NUMBER
WBS 936374.04.08.03

7. PERFORMING ORGANIZATION NAME(S) AND ADDRESS(ES)
National Aeronautics and Space Administration
John H. Glenn Research Center at Lewis Field
Cleveland, Ohio 44135-3191

8. PERFORMING ORGANIZATION REPORT NUMBER
E-16723

9. SPONSORING/MONITORING AGENCY NAME(S) AND ADDRESS(ES)
National Aeronautics and Space Administration
Washington, DC 20546-0001

10. SPONSORING/MONITORS ACRONYM(S)
NASA

11. SPONSORING/MONITORING REPORT NUMBER
NASA/TM-2008-215492

12. DISTRIBUTION/AVAILABILITY STATEMENT
Unclassified-Unlimited
Subject Category: 91
Available electronically at http://gltrs.grc.nasa.gov
This publication is available from the NASA Center for AeroSpace Information, 301-621-0390

13. SUPPLEMENTARY NOTES

14. ABSTRACT
JSC-1AF lunar simulant has been applied to AZ-93 and AgFEP thermal control surfaces on aluminum or composite substrates in a simulated lunar environment. The temperature of these surfaces was monitored as they were heated with a solar simulator and cooled in a 30 K coldbox. Thermal modeling was used to determine the absorptivity (α) and emissivity (ε) of the thermal control surfaces in both their clean and dusted states. Then, a known amount of power was applied to the samples while in the coldbox and the steady state temperatures measured. It was found that even a submonolayer of simulated lunar dust can significantly degrade the performance of both white paint and second-surface mirror type thermal control surfaces under these conditions. Contrary to earlier studies, dust was found to affect ε as well as α. Dust lowered the emissivity by as much as 16 percent in the case of AZ-93, and raised it by as much as 11 percent in the case of AgFEP. The degradation of thermal control surface by dust as measured by α/ε rose linearly regardless of the thermal control coating or substrate, and extrapolated to degradation by a factor 3 at full coverage by dust. Submonolayer coatings of dust were found to not significantly change the steady state temperature at which a shadowed thermal control surface will radiate.

15. SUBJECT TERMS
Lunar soil; Lunar dust

16. SECURITY CLASSIFICATION OF:			17. LIMITATION OF ABSTRACT	18. NUMBER OF PAGES	19a. NAME OF RESPONSIBLE PERSON
a. REPORT	b. ABSTRACT	c. THIS PAGE			STI Help Desk (email:help@sti.nasa.gov)
U	U	U	UU	21	19b. TELEPHONE NUMBER *(include area code)* 301-621-0390